Exchange-Bias Phenomenon: The Role of the Ferromagnetic Spin Structure

R. Morales,[1,2,*] Ali C. Basaran,[3] J. E. Villegas,[4] D. Navas,[5] N. Soriano,[6] B. Mora,[6] C. Redondo,[6] X. Batlle,[7] and Ivan K. Schuller[3]

[1]*Department of Chemical-Physics & BCMaterials, University of the Basque Country UPV/EHU, 48940 Leioa, Spain*
[2]*IKERBASQUE, Basque Foundation for Science, 48011 Bilbao, Spain*
[3]*Department of Physics and Center for Advanced Nanoscience, University of California San Diego,
La Jolla, California 92093, USA*
[4]*Unité Mixte de Physique CNRS/Thales, 91767 Palaiseau, France and Université Paris Sud, 91405 Orsay, France*
[5]*IFIMUP-IN and Departamento Física e Astronomia, Universidade do Porto, 4169-007 Porto, Portugal*
[6]*Department of Chemical-Physics, University of the Basque Country UPV/EHU, 48940 Leioa, Spain*
[7]*Departament de Física Fonamental and Institut de Nanociència i Nanotecnologia IN2UB, Universitat de Barcelona,
08028 Barcelona, Catalonia, Spain*

The exchange bias of antiferromagnetic-ferromagnetic (AFM-FM) bilayers is found to be strongly dependent on the ferromagnetic spin configuration. The widely accepted inverse proportionality of the exchange bias field with the ferromagnetic thickness is broken in FM layers thinner than the FM correlation length. Moreover, an anomalous thermal dependence of both exchange bias field and coercivity is also found. A model based on springlike domain walls parallel to the AFM-FM interface quantitatively accounts for the experimental results and, in particular, for the deviation from the inverse proportionality law. These results reveal the active role the ferromagnetic spin structure plays in AFM-FM hybrids which leads to a new paradigm of the exchange bias phenomenon.

Exchange coupling between dissimilar atoms has been shown as one of the fundamental interactions in governing the magnetic properties of thin film multilayers. While in magnetically hard and soft bilayers, the exchange interaction triggers springlike domain walls in the soft layer [1–4], exchange coupling gives rise to the shift of the ferromagnetic hysteresis loop along the applied magnetic field axis in antiferromagnetic-ferromagnetic (AFM-FM) systems [5,6]. The magnitude of this shift is defined as the exchange bias field (H_{EB}). The magnetic interaction between AFM and FM systems is a fundamental problem that gives information about the short-length-scale magnetic interactions in hybrids, is important for spintronics, and has received considerable attention for many years. These effects also allow reducing the writing fields in exchange spring media for magnetic storage [7], and are relevant in the design of exchange-bias-based devices such as hard drive read heads [8], spin valves [9,10], magnetic sensors [11], and spintronic devices [12,13].

Since exchange interactions are short ranged and FM domain walls are long, originally the exchange-bias phenomenon was assumed to be an interfacial effect [14]. However, recent experiments [15,16] and theories [17] have emerged which show that EB is affected by long-range interactions in the AFM. The spin structure in the bulk of the AFM has shown to be crucial determining the magnitude of H_{EB}. On the other hand, proposed theoretical models predict an inverse proportionality dependence of H_{EB} with the thickness of the FM layer, t_{FM},

$$H_{EB} = \frac{\sigma}{M_{FM} t_{FM}}, \qquad (1)$$

where σ, M_{FM}, and t_{FM}, are the interfacial exchange energy density, the FM magnetization and the FM thickness, respectively [18–20]. Experimental results have confirmed this thickness dependence in different magnetic systems [21–23], which has been taken to imply that the FM layer acts as a homogeneous macrospin and therefore EB is solely governed by the interaction at the AFM-FM interface.

Consequently, three main features characterize an exchange-bias system: (i) the spin structure of the AFM layer, (ii) the spin configuration at the AFM-FM interface, and (iii) the thickness and magnetization of the FM layer. The first two contributions set the value of σ in Eq. (1). Thus, given any magnetization M_{FM} and thickness t_{FM} for a FM material, the magnitude of H_{EB} can be predicted.

In this Letter we demonstrate that the FM spin configuration plays a crucial role in determining the magnitude of the EB field, which cannot be predicted by Eq. (1), even in case of ferromagnets thinner than the domain wall width. We unambiguously show that the inverse dependence of H_{EB} with t_{FM} is no longer satisfied under certain magnetization reversal mechanisms. This fact substantially modifies the understanding of EB and adds an extra degree of freedom for the design of EB-based devices. Furthermore, the active role of the FM domain structure not only breaks the inverse t_{FM} dependence of Eq. (1), but also gives rise to

an anomalous temperature dependence of H_{EB}. The temperature dependence of the FM spin configuration can yield an increase of H_{EB} with increasing T, contrary to standard exchange-bias systems in which the exchange coupling and therefore H_{EB} decrease with T. These findings complete the picture and show that the EB phenomenon is controlled by the AFM bulk, AFM-FM interface, and FM spin configuration. Each of these bases can be manipulated (sometimes independently) to control the magnetic properties of this hybrid.

FeF$_2$(70 nm)/NiFe (t_{FM}) bilayers capped with Al (4 nm) were deposited by electron beam evaporation at a base pressure of 2×10^{-7} Torr. Deposition temperature for FeF$_2$ was 300 °C, which grows epitaxially on top of a MgF$_2$ (110) single crystal substrate [24,25]. The FM layer, permalloy (NiFe), and the Al capping layer were deposited at 150 °C and grew textured. Six FM thicknesses (t_{FM} = 15, 30, 50, 70, 100, and 140 nm) were deposited in a single round using a stepper motor-controlled shutter, in order to avoid run-to-run differences.

Above the Néel temperature of FeF$_2$ (T_N = 78 K) permalloy layers show a well-defined easy magnetization axis parallel to the FeF$_2$ [001] crystallographic axis, which is also the AFM easy axis. All samples were saturated at 150 K in 1 kOe external magnetic field. The field was reduced to the cooling field H_{FC} = 50 Oe, and then samples were cooled down to 10 K. A magnetic hysteresis loop was measured at 10 K in a superconducting quantum interference device (SQUID). Sample temperature was raised up to 70 K at $H = 0$ and a second loop was measured at this temperature. Figure 1 shows hysteresis loops for two bilayers with 30 and 100 nm thick NiFe at 10 and 70 K, respectively. Although all samples present the same magnetic behavior for any t_{FM} at a fixed temperature, significant differences are observed when the temperature is varied. The magnetization reversal mechanism is reversible at 10 K with a progressive approach to negative saturation [Fig. 1(a)]. On the contrary, the magnetization process is irreversible at 70 K featuring square loops with a sharp magnetization reversal [Fig. 1(b)]. This remarkable difference with temperature indicates different spin configurations in the FM layer, induced by the temperature-dependent AFM-FM exchange interaction. This coupling also induces an unconventional dependence of the coercivity, which becomes null at low temperature.

Figure 2 displays the FM thickness dependence of the EB field in a logarithmic scale for 10 and 70 K. In this logarithmic scale the $H_{EB}(t_{FM})$ dependence given by formula (1) appears as a straight line with a negative slope -1. The dashed lines show this $1/t_{FM}$ dependence for different σ values. The agreement between the experimental data and the well-known Eq. (1) is excellent at 70 K. However, $H_{EB}(t_{FM})$ significantly deviates from this law at 10 K. At this temperature, if H_{EB} is fitted to Eq. (1) for the thinnest FM layers, the experimental H_{EB} gradually

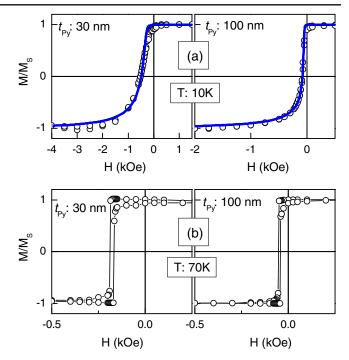diverges as t_{FM} increases, giving a much lower H_{EB} than the predicted by Eq. (1). This significant deviation is a clear proof that the EB field is not only determined by the spin configuration at the AFM-FM interface or AFM bulk, but also by the FM spin structure.

The FM spin structure not only affects the H_{EB} thickness dependence but also affects its temperature dependence. Figure 3 shows the absolute value of H_{EB} for $t_{FM} = 140$ nm. $|H_{EB}|$ monotonically increases from 10 K to a maximum at 60 K with a magnitude 36% larger than at low temperature. Then $|H_{EB}|$ decreases to zero at 78 K, the AFM Néel

FIG. 1 (color online). Hysteresis loops for FeF$_2$(70 nm)/NiFe (30 and 100 nm) bilayers at (a) $T = 10$ and (b) $T = 70$ K. Symbol: Experimental data. Blue solid line in (a): Simulation.
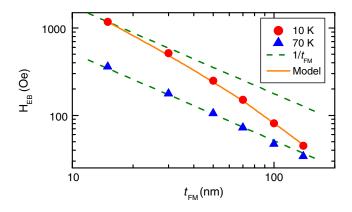

FIG. 2 (color online). FM thickness dependence of the exchange bias field for experimental data at 10 and 70 K (symbols), Eq. (1) (dashed lines), and calculated from the model in Eqs. (2)–(5) (solid line).
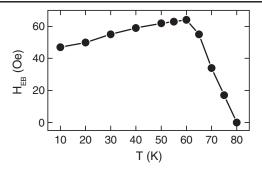
FIG. 3.   Temperature dependence of the exchange bias field for
FeF_2(70 nm)/NiFe (140 nm). Solid line is a guide for the eyes.

temperature. This result is unexpected since higher temper-
atures decrease the interfacial exchange coupling and
therefore H_{EB}, as it was observed in many EB systems,
even in bilayers using the same FeF_2 as the AFM
[15,26,27].

In order to account for these findings we propose the
model sketched in Fig. 4 [28]. It is based on Mauri´s and
Kiwi´s assumptions that allow the formation of planar
domain walls in the AFM and FM, respectively [29,30].
However, neither of these two models separately predicted
a deviation from the $1/t_{FM}$ law for H_{EB}. In our model,
domain walls parallel to the AFM-FM interface are formed
in both the AFM and FM layers. The easy axis of the
magnetic system defines the angular reference. The domain
wall in the AFM is defined by the orientation of the nearest
layer of AFM spins in contact with the FM, given by the
angle α (see Fig. 4). The FM layer is divided into N planar
"sublayers" of thickness Δt_{FM}. The magnetic moment of
each sublayer forms an angle β_i with the easy axis, with
$i = 1$ being the FM sublayer in contact with the AFM layer.
The external magnetic field is always applied along the
easy axis. The total energy of the system is given by three
contributions: the AFM domain wall energy E_{AFM}, the
exchange energy at the interface E_{AFM-FM}, and the FM
energy E_{FM}. E_{FM} includes the exchange coupling between
FM sublayers, the anisotropy energy, and the Zeeman
energy of each sublayer. Thus, the total energy per unit area
is written as

$$E = E_{AFM} + E_{AFM-FM} + E_{FM}, \qquad (2)$$

where

$$E_{AFM} = 2\sqrt{A_{AFM}K_{AFM}}(1 - \cos\alpha), \qquad (3)$$

$$E_{AFM-FM} = -J_{AFM-FM}\cos(\beta_1 - \alpha), \qquad (4)$$

$$E_{FM} = -J_{FM}\sum_{i=1}^{N-1}\cos(\beta_{i+1} - \beta_i) - K_{FM}\Delta t_{FM}\sum_{i=1}^{N}\cos^2\beta_i$$

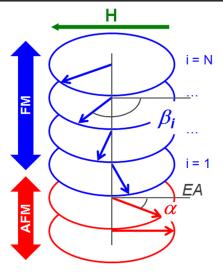$$-M\Delta t_{FM}H\sum_{i=1}^{N}\cos\beta_i. \qquad (5)$$

FIG. 4 (color online).   Schematic orientation of net magnetic
moments in AFM (red) and FM (blue) layers. The model assumes
domain walls parallel to the AFM-FM interface [28].

A_{AFM} and K_{AFM} stand for the exchange stiffness and
anisotropy constant of the AFM layers, respectively.
J_{AFM-FM} is the exchange coupling constant at the interface
while J_{FM} denotes the exchange coupling constant between
adjacent FM sublayers. K_{FM}, Δt_{FM}, and M are the FM
anisotropy constant, the FM sublayer thickness and the
magnetization of the FM material, respectively. H repre-
sents the magnitude of the applied magnetic field.

Hysteresis loops were simulated starting from positive
saturation. All β_i and α angles were calculated for each
H to minimize the total energy given by Eq. (2). The
projection of the magnetic moment of each FM slab on the
external field axis provides the contribution of the i
sublayer to the hysteresis loop. The parameters assumed
for this simulation were $A_{AFM} = 3.1 \times 10^{-8}$ erg/cm and
$K_{AFM} = 1.35 \times 10^8$ erg/cm^2 from Refs. [31,32], $J_{AFM-FM} =$
2 erg/cm^2 and $J_{FM} = 18$ erg/cm^2 were adjusted to fit all
$M(H)$ curves, $K_{FM} = 4 \times 10^3$ erg/cm^3 was obtained from
the saturation field along the hard axis of the FM layer, and
the permalloy magnetization was $M_{NiFe} = 800$ emu/cm^3.
The thickness of each FM sublayer, Δt_{FM}, was fixed to
1 nm. All parameters were kept constant for all FM
thicknesses and only the number of sublayers N was varied
to obtain the total FM thickness, $t_{FM} = N \Delta t_{FM}$.

Simulated $M(H)$ curves (solid blue lines) are compared
to experimental data at low temperature (10 K) in Fig. 1(a)
for $t_{FM} = 30$ and 100 nm. The simulation fits very well
the shape of the hysteresis loops with a fast decay of the
magnetization approaching the exchange-bias field and a
slow saturation at negative fields. The model predicts a
reversible magnetization reversal mechanism even for the
thickest sample, $t_{FM} = 140$ nm, which was confirmed by
SQUID measurements.

The theoretical dependence $H_{EB}(t_{FM})$ extracted from
the simulated $M(H)$ curves is compared to experimental

values at 10 K in Fig. 2. The agreement is excellent, predicting the quantitative deviation of the EB field from the inverse proportionality model (dashed line). This proves that the in-depth FM spin configuration induced by exchange interaction is responsible for the deviation in the magnitude of the EB field.

Incomplete domain walls were experimentally proven in exchange-coupled systems by the magneto-optical Kerr effect [24], soft-x-ray scattering, and polarized neutron reflectivity [33,34]. The theoretical behavior of this spin structure was studied by Mejia-Lopez et al. [35], who developed an analytical expression for the H_{EB} thickness dependence of incomplete domain walls. A crossover from $1/t_{FM}$ for thin films to $1/(t_{FM})^{1.9}$ for thick FM films was predicted. However, no experimental deviation from $1/t_{FM}$ was theoretically or experimentally reported for t_{FM} smaller than the FM domain wall width. In order to observe such a deviation, the FM material must be magnetically very soft. We have also investigated FeF_2/Ni bilayers (not shown). In this case, the deviation from the $1/t_{FM}$ law for thick Ni is much smaller than for NiFe.

At higher temperature the reversal mechanism is different. There are no domain walls parallel to the AFM-FM interface. The square shape of the hysteresis loops at 70 K suggests the reversal mechanism goes through a nucleation of opposite FM domains with domain walls perpendicular to AFM-FM interface, followed by a domain wall motion as H increases. This domain structure in the FM layer yields a $1/t_{FM}$ dependence as shown in Fig. 2 at 70 K, and as it has been proved in many other systems [36].

The thermal evolution of the FM spin structure explains the anomalous H_{EB} temperature dependence of Fig. 3. At low temperature the magnetization reversal occurs by incoherent rotation of the planar FM sublayers, creating a springlike domain wall parallel to the AFM-FM interface. This FM spin configuration yields a much lower H_{EB} than the value predicted by Eq. (1). This deviation increases with t_{FM}, since the springlike domain wall widely extends with a larger difference between β_N and β_1 (see Fig. 4). However, the magnetization reversal at higher temperature is dominated by nucleation of inverse domains and domain wall motion. This mechanism follows formula (1), leading to a higher magnitude of H_{EB} with respect to the parallel domain wall mechanism. Consequently, H_{EB} increases with temperature as the FM spin configuration evolves between these two mechanisms. Another possible scenario for the thermal dependence was studied by Billoni et al. [37]. They predicted, by Monte Carlo simulations and assuming a coherent rotation mechanism, the appearance of coercivity at higher temperature, close to T_N. However, this mechanism yields lower blocking temperatures, T_B, and a monotonous decrease of H_{EB}. We have not observed any of these two effects in our system. It is worth mentioning that the exchange interaction decreases as temperature increases. Thus, a reduced value of H_{EB} is expected as

temperature rises. However, the thermal evolution of the FM spin structure can overturn this trend.

In conclusion, the FM spin configuration affects the magnitude of H_{EB}. The broken inverse proportionality of $H_{EB}(t_{FM})$ and the enhancement of H_{EB} at higher temperature reveal the importance of the FM spin structure in the EB phenomenon, and expand the overview of this phenomenon in FM films thinner than the FM correlation length. Therefore, a general understanding of exchange bias must take into account three pillars: the pinned spin distribution at the AFM-FM interface, the pinned spin distribution in the AF bulk and the FM spin configuration. The latter is an important ingredient which cannot be ignored for the development of EB theories. Moreover, these results imply that complex FM spin textures, as skyrmions or magnetic topological defects [38–40] may also show unpredicted dependences when exchange coupled to antiferromagnetic or large anisotropic materials. The active role of the FM spins should also be considered in the design of exchange coupling-based devices or hard and soft heterostructures for ultrahigh density storage media.

---

*rafael.morales@ehu.es

[1] E. E. Fullerton, J. S. Jiang, M. Grimsditch, C. H. Sowers, and S. D. Bader, Phys. Rev. B **58**, 12193 (1998).

[2] P. Steadman, M. Ali, A. T. Hindmarch, C. H. Marrows, B. J. Hickey, S. Langridge, R. M. Dalgliesh, and S. Foster, Phys. Rev. Lett. **89**, 077201 (2002).

[3] Y. Henry, S. Mangin, T. Hauet, and F. Montaigne, Phys. Rev. B **73**, 134420 (2006).

[4] G. Guo, G. Zhang, and X. Wang, J. Appl. Phys. **108**, 043919 (2010).

[5] W. H. Meiklejohn and C. P. Bean, Phys. Rev. **105**, 904 (1957).

[6] J. Nogués and I. K. Schuller, J. Magn. Magn. Mater. **192**, 203 (1999).

[7] D. Suess, T. Schrefl, S. Fahler, M. Kirschner, G. Hrkac, F. Dorfbauer, and J. Fidler, Appl. Phys. Lett. **87**, 012504 (2005).

[8] S. Parkin, X. Jiang, C. Kaiser, A. Panchula, K. Roche, and M. Samant, Proc. IEEE **91**, 661 (2003).

[9] M. Bonfim, G. Ghiringhelli, F. Montaigne, S. Pizzini, N. B. Brookes, F. Petroff, J. Vogel, J. Camarero, and A. Fontaine, Phys. Rev. Lett. **86**, 3646 (2001).

[10] B. G. Park, J. Wunderlich, X. Martí, V. Holý, Y. Kurosaki, M. Yamada, H. Yamamoto, A. Nishide, J. Hayakawa, H. Takahashi, A. B. Shick, and T. Jungwirth, Nat. Mater. **10**, 347 (2011).

[11] B. Negulescu, D. Lacour, F. Montaigne, A. Gerken, J. Paul, V. Spetter, J. Marien, C. Duret, and M. Hehn, Appl. Phys. Lett. **95**, 112502 (2009).

[12] T. N. A. Nguyen, Y. Fang, V. Fallahi, N. Benatmane, S. M. Mohseni, R. K. Dumas, and J. Akerman, Appl. Phys. Lett. **98**, 172502 (2011).

[13] T. Gasi, A. K. Nayak, J. Winterlik, V. Ksenofontov, P. Adler, M. Nicklas, and C. Felser, Appl. Phys. Lett. **102**, 202402 (2013).

[14] W. H. Meiklejohn, J. Appl. Phys. **33**, 1328 (1962).

[15] R. Morales, Z.-P. Li, J. Olamit, K. Liu, J. M. Alameda, and I. K. Schuller, Phys. Rev. Lett. **102**, 097201 (2009).

[16] M. Y. Khan, C.-B. Wu, and W. Kuch, Phys. Rev. B **89**, 094427 (2014).

[17] P. Miltényi, M. Gierlings, J. Keller, B. Beschoten, G. Güntherodt, U. Nowak, and K. D. Usadel, Phys. Rev. Lett. **84**, 4224 (2000).

[18] A. E. Berkowitz and K. Takano, J. Magn. Magn. Mater. **200**, 552 (1999).

[19] R. L. Stamps, J. Phys. D **33**, R247 (2000).

[20] M. Kiwi, J. Magn. Magn. Mater. **234**, 584 (2001).

[21] S. M. Zhou, K. Liu, and C. L. Chien, J. Appl. Phys. **87**, 6659 (2000).

[22] M. Gruyters and D. Riegel, Phys. Rev. B **63**, 052401 (2000).

[23] C. Leighton, M. R. Fitzsimmons, A. Hoffmann, J. Dura, C. F. Majkrzak, M. S. Lund, and I. K. Schuller, Phys. Rev. B **65**, 064403 (2002).

[24] R. Morales, Z.-P. Li, O. Petracic, X. Batlle, I. K. Schuller, J. Olamit, and K. Liu, Appl. Phys. Lett. **89**, 072504 (2006).

[25] M. R. Fitzsimmons, B. J. Kirby, S. Roy, Z.-P. Li, I. V. Roshchin, S. K. Sinha, and I. K. Schuller, Phys. Rev. B **75**, 214412 (2007).

[26] M. Grimsditch, A. Hoffmann, P. Vavassori, H. Shi, and D. Lederman, Phys. Rev. Lett. **90**, 257201 (2003).

[27] I. V. Roshchin, O. Petracic, R. Morales, Z.-P. Li, X. Batlle, and I. K. Schuller, Europhys. Lett. **71**, 297 (2005).

[28] For clarity, and general purpose, Fig. 4 sketches a ferromagnetic coupling between AFM and FM layers. However, the $FeF_2 - Ni$ coupling is antiferromagnetic. This fact does not affect the calculation, since the sign of E_{AFM-FM} [Eq. (4)] remains the same—both J_{AFM-FM} and $\cos(\beta_1 - \alpha)$ have opposite sign to the ferromagnetic coupling case.

[29] D. Mauri, H. C. Siegmann, P. S. Bagus, and E. Kay, J. Appl. Phys. **62**, 3047 (1987).

[30] M. Kiwi, J. Mejía-López, R. D. Portugal, and R. Ramírez, Europhys. Lett. **48**, 573 (1999).

[31] J. Nogués, D. Lederman, T. J. Moran, I. K. Schuller, and K. V. Rao, Appl. Phys. Lett. **68**, 3186 (1996).

[32] Z.-P. Li, C. W. Miller, I. V. Roshchin, and I. K. Schuller, Phys. Rev. B **76**, 014423 (2007).

[33] S. Roy, M. R. Fitzsimmons, S. Park, M. Dorn, O. Petracic, I. V. Roshchin, Z.-P. Li, X. Batlle, R. Morales, A. Misra, X. Zhang, K. Chesnel, J. B. Kortright, S. K. Sinha, and I. K. Schuller, Phys. Rev. Lett. **95**, 047201 (2005).

[34] S.-W. Chen, X. Lu, E. Blackburn, V. Lauter, H. Ambaye, K. T. Chan, E. E. Fullerton, A. E. Berkowitz, and S. K. Sinha, Phys. Rev. B **89**, 094419 (2014).

[35] J. Mejia-Lopez, R. Ramirez, and M. Kiwi, J. Magn. Magn. Mater. **241**, 364 (2002).

[36] V. I. Nikitenko, V. S. Gornakov, A. J. Shapiro, R. D. Shull, K. Liu, S. M. Zhou, and C. L. Chien, Phys. Rev. Lett. **84**, 765 (2000).

[37] O. V. Billoni, A. Cannas, S, and F. A. Tamarit, J. Phys. Condens. Matter **23**, 386004 (2011).

[38] X. Z. Yu, Y. Onose, N. Kanazawa, J. H. Park, J. H. Han, Y. Matsui, N. Nagaosa, and Y. Tokura, Nature **465**, 901 (2010).

[39] M. Ezawa, Phys. Rev. Lett. **105**, 197202 (2010).

[40] A. Hierro-Rodriguez, M. Vélez, R. Morales, N. Soriano, G. Rodríguez-Rodríguez, L. M. Álvarez-Prado, J. I. Martín, and J. M. Alameda, Phys. Rev. B **88**, 174411 (2013).